ORIGINAL PAPER

Spatiotemporal variability of vegetation due to drought dynamics (2012–2017): a case study of the Upper Paraíba River basin, Brazil

Glauciene Justino Ferreira da Silva[1] · Nádja Melo de Oliveira[1] ·
Celso Augusto Guimarães Santos[2] · Richarde Marques da Silva[3]

Abstract

Vegetation indices have been widely used for monitoring the spatiotemporal variables of vegetation and characterizing droughts, primarily in semiarid regions. Drought is a multifaceted natural process that can lead to reduced water availability and can consequently have extensive effects on the socioeconomic, agricultural and development sectors of countries. This study aims to evaluate the spatial–temporal pattern of vegetation as a result of drought dynamics during the last major drought (2012–2017) in the Brazilian semiarid region. Satellite image products from the Moderate Resolution Imaging Spectroradiometer (MOD16, MOD11 and MOD15), standardized precipitation index, rainfall anomaly and vegetation indices were used to monitor and identify drought episodes. To relate vegetation with droughts, the vegetation supply water index was used. The results revealed a strong influence of droughts on vegetation behavior and a strong seasonal pattern of variables in the study area, primarily for land surface temperature, leaf area index and evapotranspiration. These results lead to the conclusion that, based on correlations between vegetation and droughts over a climatological period, it is possible to evaluate the relative roles of vegetation behavior for semiarid regions using MODIS products.

✉ Celso Augusto Guimarães Santos
celso@ct.ufpb.br

1 Postgraduate Program, Civil and Environmental Engineering/CT/UFPB, Federal University of Paraíba, João Pessoa, PB 58051-900, Brazil

2 Department of Civil and Environmental Engineering, Federal University of Paraíba, João Pessoa, PB 58051-900, Brazil

3 Department of Geosciences, Federal University of Paraíba, João Pessoa, PB 58051-900, Brazil

Graphic abstract
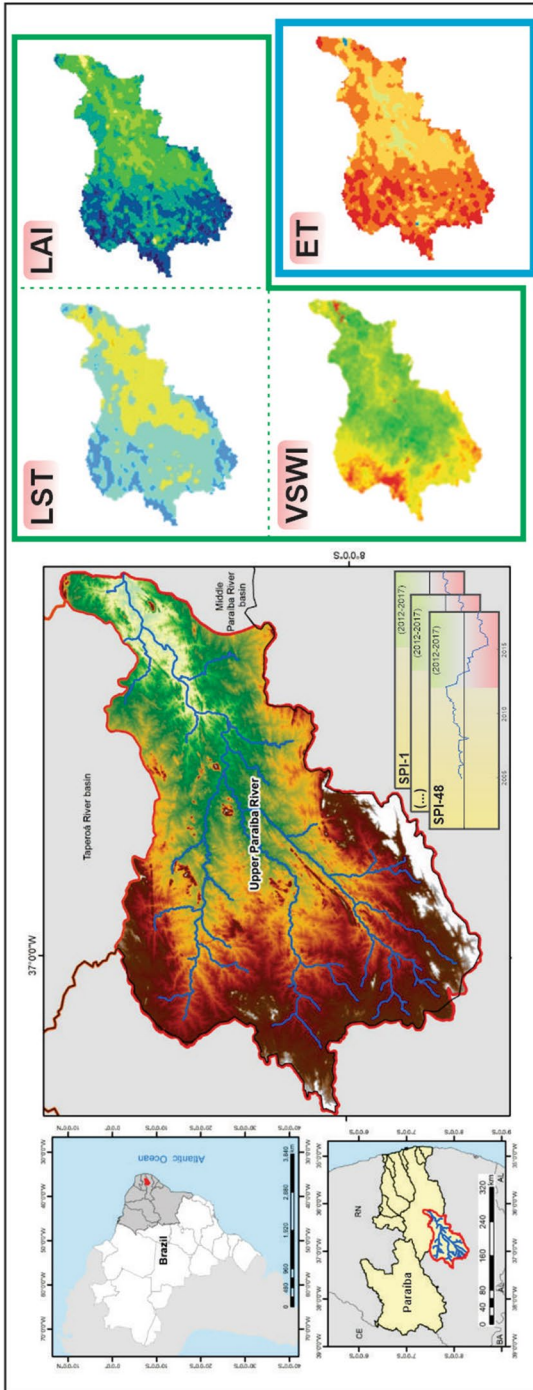
1 Introduction

Droughts are an important factor in vegetation behavior in the Brazilian semiarid region due to a thin soil layer, crystalline basement and constant water scarcity. The Brazilian semiarid region has experienced recurrent drought periods throughout its history, which promote several social and economic problems in the region, especially in arid or semiarid regions (Gutiérrez et al. 2014). In Brazil, from 1980 to 2010, approximately 15% of natural disasters were related to drought phenomena in Northeast Brazil (NEB) (Cunha et al. 2015).

In NEB, the indiscriminate use of natural resources for agricultural purposes, urban expansion and economic activities, and unplanned human activities have been the subject of constant debate due to the environmental problems that they cause (Hunt et al. 2018). In this sense, an analysis of biophysical variables can help diagnose the changes that occur in this environment, because they significantly express changes caused by land use and by droughts (Mariano et al. 2018).

Some of these variables such as drought index, land surface temperature and vegetation indices have been applied (Gomes et al. 2017; Xie et al. 2019; Ma et al. 2019; García-León et al. 2019), but few studies have analyzed evapotranspiration (ET) behavior in the different soil covers in the semiarid region of NEB (Anderson et al. 2016; Heinemann et al. 2017), especially during the most recent drought (2012–2017), which is considered to be one of the most severe in this region (Marengo et al. 2017; De Azevedo et al. 2018). In semiarid regions, where environmental characteristics differ due to water scarcity, a spatiotemporal analysis of these variables is essential to conduct environmental diagnoses and provide relevant information on environmental degradation in the region.

More recently, with technological advances in the preceding decades and the availability of orbital data for civil society, research on this topic has gained prominence and has addressed several biomes and different terrestrial ecosystems (Beuchle et al. 2015). Among the sensors recently launched on board remote sensing satellites, the Moderate Resolution Imaging Spectroradiometer (MODIS) offers a range of products for the greatest variety of studies on the phenomena that occur at the Earth's surface (Cunha et al. 2015; Silva et al. 2019; Li et al. 2019).

In this sense, several studies have been developed with this purpose; however, studies of the Brazilian semiarid region remain scarce. Regional studies include that by Cunha et al. (2017), who evaluated a methodology to monitor drought impacts on pasture areas in the Brazilian semiarid region using normalized difference vegetation index (NDVI) and land surface temperature (LST) data, as well as Brazilian Institute of Geography and Statistics (IBGE) secondary data, Awange et al. (2016) analyzed droughts in Brazil for the period from 1901 to 2013 using precipitation data in a 25 km×25 km grid; and Cunha et al. (2015) monitored vegetation drought dynamics in the Brazilian semiarid region using only vegetation indices and soil temperature for the years 2012 and 2013, i.e., for the beginning of the drought period. In contrast, the present study analyzes the spatial and temporal variability of vegetation as a result of drought dynamics between 2012 and 2017 for different typologies of vegetation cover of a Brazilian semiarid basin. The mean annual rainfall in
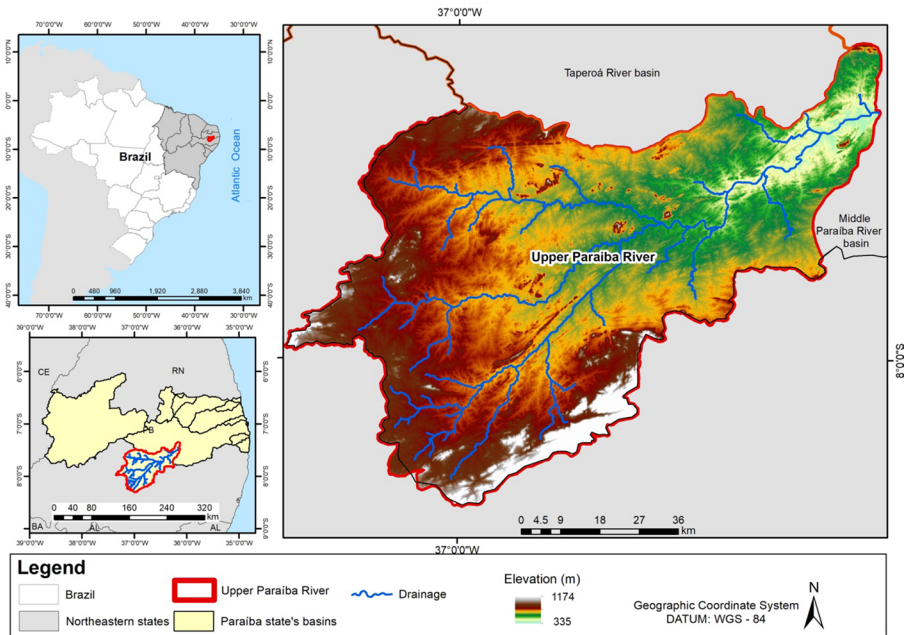
Fig. 1 Location of the Upper Paraíba River basin in the Northeast Brazil

this region decreased from 515 mm (1994–2011) to 290 mm (2012–2017), as shown by De Medeiros et al. (2019). Such a reduction in the mean annual precipitation had severe impacts on the water supply of the Epitácio Pessoa dam, one of the major reservoirs in the semiarid region of Paraíba State, which provides water to 500,000 Campina Grande residents and several other cities of Paraíba State (Silva 2019). From 2012 to 2017, expressive precipitation deficits were registered in addition to the two anomalous high-pressure centers over the region that enabled the occurrence of extreme drought events (in terms of both impacts and people affected) (Marengo et al. 2017; Brito et al. 2018). As a result, severe policies of water rationing were implanted to supplement the water supply to meet consumption.

Thus, the present study analyzes in an integrated manner the LST, ET, leaf area index (LAI) and precipitation for the entire drought period, i.e., 2012–2017. In light of the above, this study aims to evaluate the spatial and temporal pattern of vegetation during the drought period between 2012 and 2017 for the Upper Paraíba River basin, in the semiarid region of Brazil, using MODIS sensor products (MOD16, MOD11 and MOD15).

2 Materials and methods

2.1 Study area

The Upper Paraíba River basin is located in the semiarid region in Paraíba State, specifically, between 06° 00′ 11′ and 08° 19′ 54″ south and 34° 45′ 50″ and 38° 47′ 58″ west (Fig. 1). The local climate of the Upper Paraíba River basin, according to the Köppen classification,
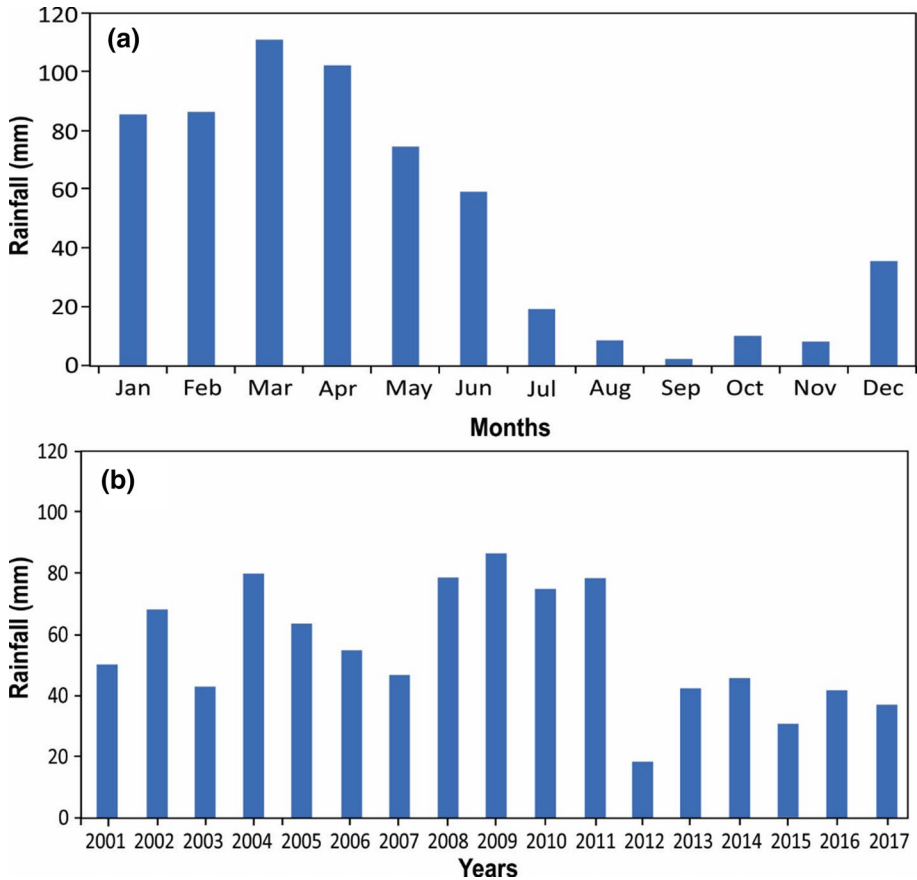
Fig. 2 a Monthly rainfall variation and **b** annual rainfall variation for the Upper River Paraíba basin between 2012 and 2017

is BSh—with a low latitude and altitude (Alvares et al. 2013). The mean annual precipitation ranges from 400 to 600 mm (Fig. 2a), and the dry season lasts from 8 to 10 months, with rainfall concentrated between January and May, corresponding to 65% of the annual rainfall (Fig. 2b), and with high mean temperatures above 28 °C (Dantas et al. 2015). The local biome is the caatinga (semiarid vegetation), which is a heterogeneous biome consisting of a mosaic of shrubs and seasonally dry forest areas (Santos et al. 2017), occurring primarily under semiarid conditions.

The geology of the basin is composed primarily of crystalline rocks that comprise the Precambrian Shield of Northeast Brazil. Vegetation in the basin consists predominantly of small caatinga vegetation, including the presence of cochineal cactus, cotton and agave crops, as well as temporary corn and bean crops, which represent a small area of the basin (Beuchle et al. 2015).

The semiarid region of Brazil corresponds to an area located predominantly in NEB (including the municipalities of the northern portion of Minas Gerais state but excluding Maranhão state), which has the following characteristics: (a) mean annual rainfall of less than or equal to 800 mm; (b) an aridity index as high as 0.5, calculated by the water balance, which

relates to the rainfall and ET potential between 1961 and 1990; and (c) a drought risk greater than 60%, calculated for the period between 1970 and 1990 (Brazil 2017). This portion of the Brazilian territory occupies an area of 969,589 km^2, with a population of approximately 24 million inhabitants, and is historically subject to the effects of drought and the challenges associated with accessing available water in the region, resulting in the construction of several hydraulic projects to reduce the effects of water scarcity (Alvalá et al. 2017).

2.2 Rainfall data

Because the rain gauge network in the Upper Paraíba River basin has a poor spatial distribution and many missing data in its historical series, Tropical Rainfall Measuring Mission (TRMM) data were used here to analyze the rainfall anomaly. Satellite data using spaceborne sensors provide an excellent complement to capture continuous rainfall events at various spatial and temporal scales. Thus, the TRMM data (Kummerow et al. 1998, 2000; Huffman and Bolvin 2017) provide an accurate alternative source of rain data at fine spatiotemporal resolution. The accuracy of the TRMM data has already been tested in several studies in many countries (Santos et al. 2018; Fang et al. 2019; Gadelha et al. 2019; Kalimeris and Kolios 2019) as well as in the region of Upper Paraíba River basin (Diniz et al.2016; Silva et al. 2018; Santos et al. 2019a,b). The rainfall data used in this study originated from the TRMM satellite, obtained from algorithm 3B42 version 7 using a spatial resolution of 0.25°×0.25° from January 2012 to December 2017, with total coverage of the Upper Paraíba study area composed of a grid of 42 cells.

2.3 Determination of the rainfall anomaly index (RAI)

The RAI was used to analyze rainfall anomalies by estimating the frequency and intensity of dry and rainy years (Table 1) in the Upper Paraíba River basin. In addition, the monthly RAI was calculated for specific years of the historical series to analyze the rainfall distribution in the years of greatest anomaly. The RAI was developed by Van Rooy (1965) and adapted by Kraus (1977) and is calculated as:

$$\text{RAI} = 3 \left[\frac{\left(N - \overline{N} \right)}{\left(\overline{M} - \overline{N} \right)} \right] \quad \text{for positive anomalies} \tag{1}$$

Table 1 Rainfall anomaly index (RAI) intensity classes

Values	Intensity
>4	Extremely humid
2 to 4	Very humid
0 to 2	Humid
−2 to 0	Dry
−4 to−2	Very dry
<−4	Extremely dry

$$\text{RAI} = -3 \left[\frac{\left(N - \overline{N} \right)}{\left(\overline{X} - \overline{N} \right)} \right] \quad \text{for negative anomalies} \tag{2}$$

where N = current monthly/yearly rainfall, i.e., the month/year when the RAI will be generated (mm); $\overline{N}$ = monthly/yearly average rainfall of the historical series (mm); M = average of the ten highest monthly/yearly rainfall events of the historical series (mm); X = average of the ten lowest monthly/yearly precipitation events of the historical series (mm); and positive anomalies have values that are above average, and negative anomalies have values that are below average.

To use this index, the rainfall data obtained by the TRMM had to be prepared. The TRMM data were processed and organized into monthly averages. To determine whether the anomaly was positive or negative, an average was calculated for each year, obtained by subtracting the standard deviation. Thus, positive anomalies represented above-average values and negative anomalies represented below-average values.

After analyzing the annual and monthly precipitation and obtaining the RAI values in relation to precipitation for the period 2012–2017, the results were plotted in a spatial distribution map in the ArcMap® 10.1 software, using the Kriging method.

2.4 Drought assessment using the SPI

To calculate the standardized precipitation index (SPI) (McKee et al. 1993) over the region, the TRMM precipitation data were used. The SPI is used to monitor meteorological droughts, and in the present study, it was calculated on 1-, 3-, 6-, 9-, 12-, 18-, 24-, 48-month scales, which also allowed the evaluation of agricultural droughts. The SPI is used to monitor meteorological drought and in this study was computed over short to long temporal scales (i.e., from 1 to 48 months), making it possible to evaluate annual conditions of precipitation and to thus describe the different impacts related to water supply. The basis of the calculation is long-term precipitation data that are fitted to a probability distribution transformed into a normal distribution. The normal distribution provides a way to identify the frequency of the drought classifications. For any location, the SPI analysis through several timescales is adequate to verify hydrological drought and applications. The negative part of the SPI range is arbitrarily divided into four categories, i.e., mildly dry $(0 > \text{SPI} > -0.99)$, moderately dry $(-1.0 > \text{SPI} > -1.49)$, severely dry $(-1.5 > \text{SPI} > -1.99)$ and extremely dry conditions (SPI less than -2.0).

Table 2 MODIS products used in the study

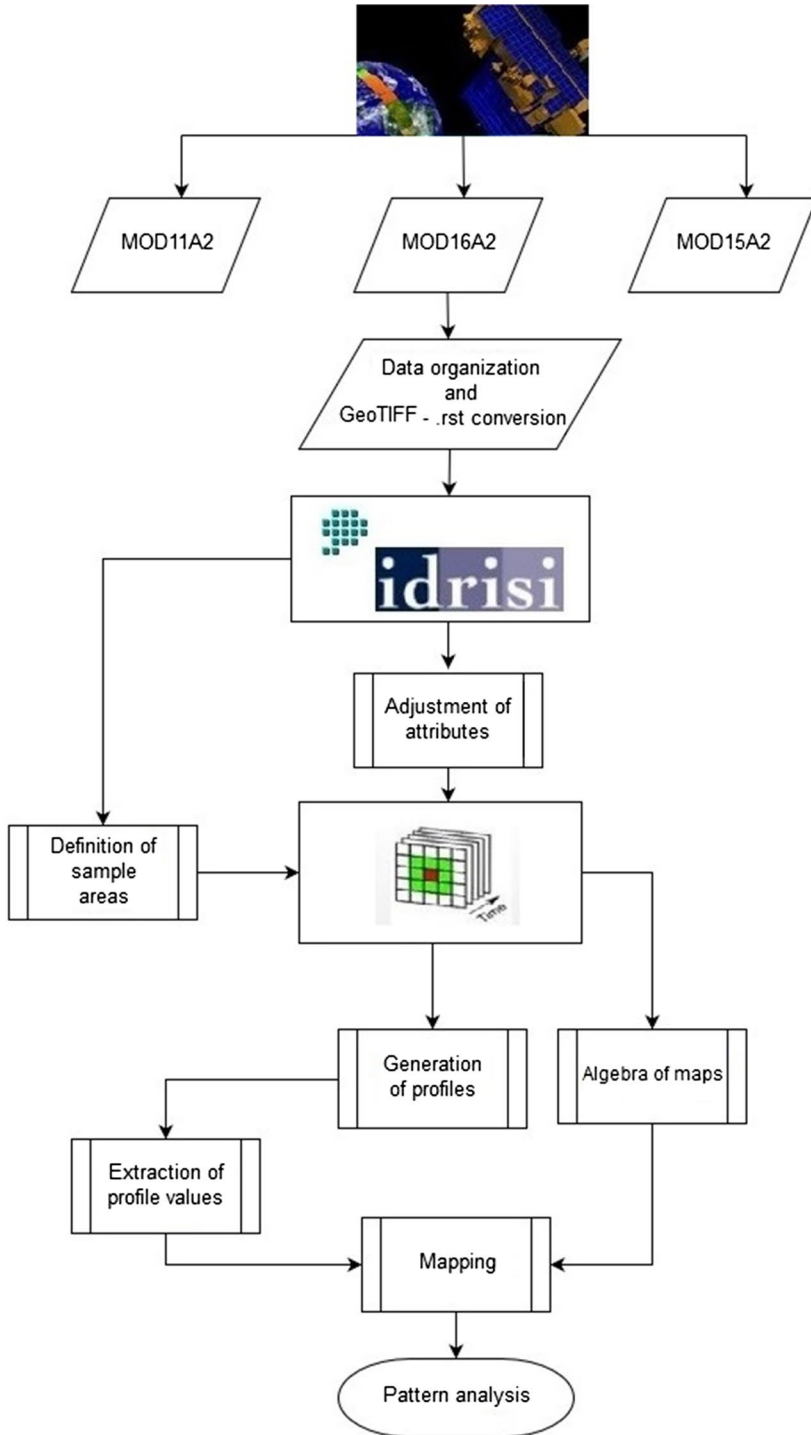| Product	Period	Spatial resolution	Temporal resolution
MOD16A2	01/01/00 to 12/27/14	1 km	8 days
MOD11A2 Day	03/05/00 to 10/16/15	1 km	Daily
MOD15A2	02/26/00 to 10/16/15	250 m	8 days

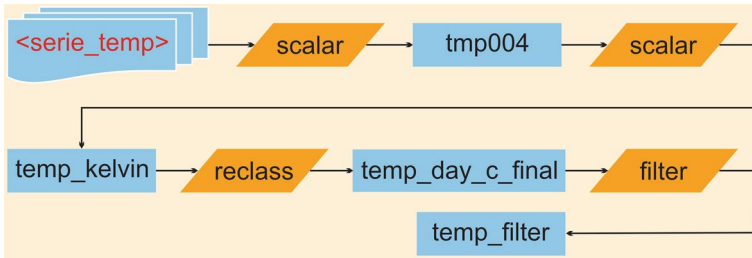**Fig. 3** Flowchart of the adopted methodological procedures

Fig. 4 Example sequence used for adjusting the LST series used in this study

2.5 NDVI and LST

To analyze the vegetation behavior, NDVI and LST were applied. At this stage, the MODIS/TERRA sensor products were used, which are freely available at: https://daac.ornl.gov/cgi-bin/MODIS/GLBVIZ_1_Glb/modis_subset_order_global_col5.pl; this Web site provides the images in GeoTIFF format and geographic coordinate systems without the need for conversions (Table 2). IDRISI Kilimanjaro software was used for image processing and information extraction, as well as spatial analysis and map algebra operations. Finally, ArcGIS 10.1 software was used to create the maps.

The methodological procedures for applying these two indices are described in Fig. 3. The first step in the processing of the MODIS images was selecting existing products in the period 2012–2017, using *Tile* h14v09 in a sample area of 101×101 km. After this step, a Fortran language program was created to convert the GeoTIFF images to IDRISI Raster Format (.rst), followed by an import of files and generation of a time series in IDRISI using the *Collection Editor* tool (Fig. 4). After the time series (LST, ET and LAI) were generated, it was possible to generate models in the *Macro Modeler* menu of IDRISI to adjust the required parameters.

The LST and NDVI images were obtained through the link: https://modis.ornl.gov/cgi-bin/MODIS/GLBVIZ_1_Glb/modis_subset_order_global_col5.pl. To obtain the NDVI products with their normalized values, the values had to be multiplied by the scale
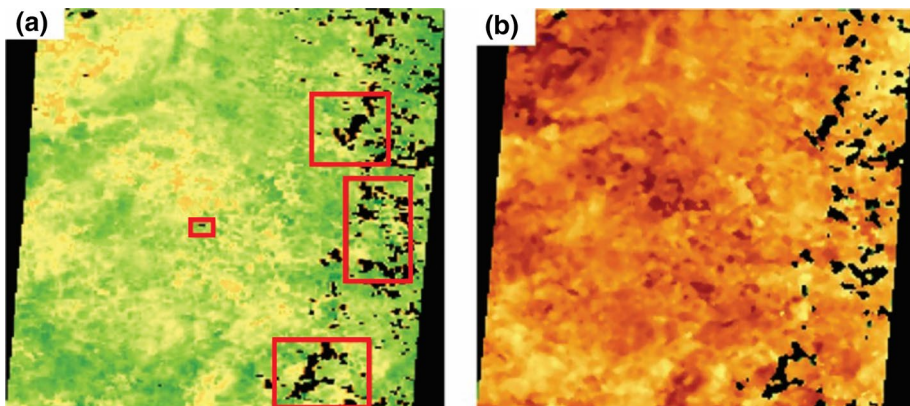

Fig. 5 **a** LST image with noise and **b** LST image after application of mode 3×3 filter

factor 0.0001, whereas a factor of 0.02 was used for the LST products, both of which were adopted from the MODIS product manual. Then, the LST images were converted from Kelvin to Celsius. LST and NDVI images with negative values were adjusted to zero. In the LST image, pixel resampling was performed for a spatial resolution of 250 m, obtaining NDVI and LST products with similar spatial resolutions.

The MOD11A2 product contains LST data produced by the MODIS sensor using the *Day/Night LST* algorithm developed specifically for this sensor, which produces daytime and nighttime thermal images. In this study, the daytime LST product was used.

Finally, pixels (area highlighted in Fig. 5a) with zero values distributed and concentrated in the images, characteristic of image-related noises and noise caused by atmospheric, radiometric or geometric factors, were observed. To improve the LST images, IDRISI filters were applied to all images. The filter with the best results was mode 3×3. Figure 5b depicts an image of LST after application of the aforementioned filter.

2.6 Determining LAI for vegetation monitoring

MODIS product data have been used to present global LAI values since 2000 (Myneni et al. 2002). The quality of these products varies, primarily due to cloud cover, instrument issues, missing data and other noises (Xiao et al. 2009; Jiang et al. 2010). Time series of LAI provide data on seasonal vegetation development and support analyses of the functional and structural characteristics of global and regional land cover types. To determine the LAI in this study, the MOD15A2 product, which contains information on LAI and photosynthetically active radiation fractions, was used. This product has a 1-km spatial resolution and 8-day temporary resolution. Because this original product has "gaps" in pixels, we preprocessed the data using the 3×3 mode filtering algorithm to generate a continuous time series. Then, a second reclassification was performed, because for caatinga vegetation in the study area, all LAI values greater than 6 were removed from the series.

Fig. 6 Sample areas of three types of caatinga vegetation present in the Upper Paraíba River basin
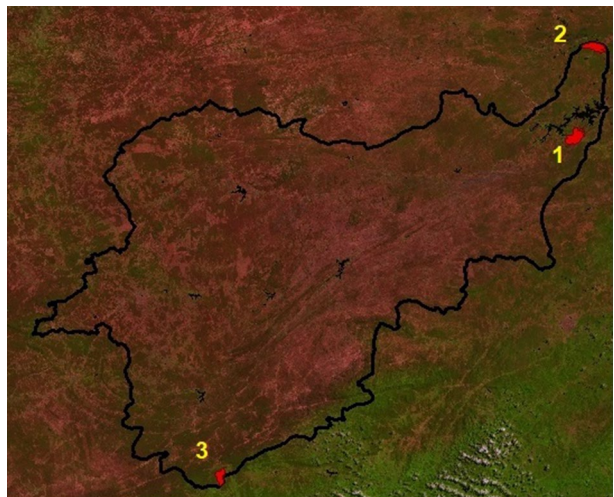
2.7 Definition of sample areas and profile of the created time series

To analyze vegetation behavior, three sample areas were defined (Fig. 6), based on three caatinga vegetation strata: (1) shrub vegetation, (2) tree vegetation and (3) shrub-tree vegetation. These areas were selected because their characteristics are known due to previous field work in those areas.

For generation of the temporal profiles using the profile function of the IDRISI software, the files with time series (LST, LAI and ET) and images of the study area and vegetation samples were used. For both the profile of the basin area analyzed and the profile of the vegetation sample areas, the average was chosen for extraction of the values. The mean values of each series were plotted for each sample area, to analyze the behavior of the variables in each vegetation stratum.

2.8 Vegetation supply water index (VSWI) estimation

To analyze the vegetation dynamics during the severe drought period, the VSWI developed by Carlson et al. (1994) was applied. The VSWI indicates the drought condition, the water stress in the vegetation and the humidity and areas affected by the drought (Zhou et al. 2013). The VSWI was obtained using MODIS NDVI (MOD13Q1) images for 16-day intervals at 250-m resolution, as well as the MODIS 8-day LST (MOD11A2) product at 1-km resolution, both from collection 6, for the 2012–2017 period. High VSWI values indicate a low temperature and/or high vegetative vigor, indicating vegetation without water stress, whereas a small VSWI value implies that the temperature of the vegetation is high or that the vegetative vigor is low, resulting in a water stress condition. This index is inversely proportional to the moisture content in the soil and indirectly indicates the water supply to the vegetation. The VSWI is calculated as:

$$\text{VSWI} = \frac{\text{NDVI}}{\text{LST}} \tag{3}$$

In this study, the modified VSWI was used for drought monitoring based on the proposal of Cunha et al. (2015). According to the literature, drought is apparent when the VSWI threshold value exceeds 60, and the drought severity decreases when the values are below 60. However, this threshold may vary depending on different factors, including vegetation cover, vegetation type, local climatic conditions and soil type. Thus, to avoid using a threshold that may contain errors, the study considered the VSWI anomaly percentage (VSWI$_{anom\%}$), which is used to compare a period of the index with an average of several years, obtained by the equation:

$$\text{VSWI}_{anom\%} = \frac{\text{VSWI} - \overline{\text{VSWI}}}{\overline{\text{VSWI}}} \times 100 \tag{4}$$

2.9 ET-monitoring products

To estimate ET, the MOD16A2 product was used, which is a revision of the algorithm proposed by Cleugh et al. (2007). This product adapted the Penman–Monteith equation for use with remote sensing data. For the series of MOD16A2 images of the study area, Macro Modeler was used to rescale the images, multiplying the series by a factor of 0.1.
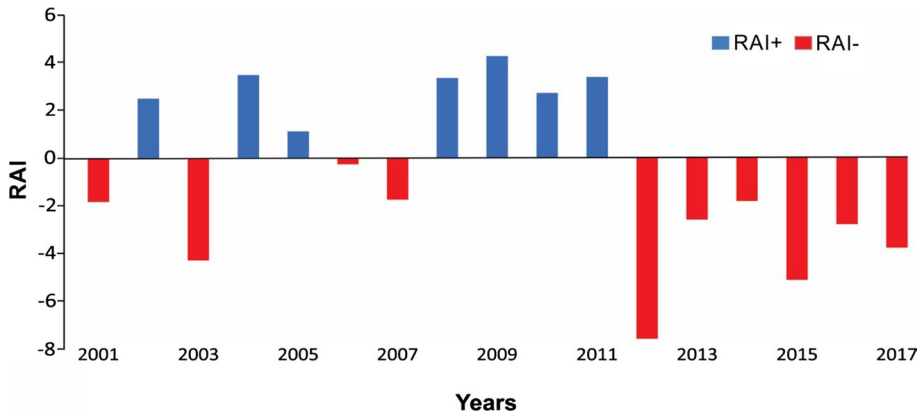
Fig. 7 Temporal distribution of the RAI for the Upper Paraíba River basin between 2001 and 2017

Following that procedure, the series was reclassified to remove values greater than 10 mm/day, because daily ET values do not exceed this value for the study area. Data were checked for errors, and erroneous values were replaced with the preceding and subsequent values that met the quality control criteria, similar to the approach followed with the LST and LAI products. These 8-day products were then interpolated to provide daily values used to calculate the daily surface conductance, to match the daily time step of the meteorological forcing data.

3 Results and discussion

3.1 Analysis of droughts and water deficits

Figure 7 shows the temporal distribution of the RAI for the Upper Paraíba River basin. The RAI was applied for the analysis of water scarcity in the basin area in the period 2001–2017. The results obtained from this index reveal that the highest occurrences were in the years classified as being very dry (2013, 2016 and 2017), followed by the years 2012 and 2015, which were classified as being extremely dry (Table 2). The results show that the years between 2012 and 2015 had an RAI between -2 and -8, different from previous years (2001–2011), when only two years had values of approximately -2, revealing a significant discrepancy between these two periods.

Table 3 RAI classification for the Upper Paraíba River basin

Values	Intensity	Years
≥ 4	Extremely humid	–
2 to 4	Very humid	–
0 to 2	Humid	–
0 to -2	Dry	2014
-2 to -4	Very dry	2013, 2016, 2017
≤ -4	Extremely dry	2012, 2015

The rainfall in NEB results from the influence of several atmospheric factors at several scales, such as the upper tropospheric cyclonic vortices, intertropical convergence zone, frontal systems and eastern disturbances (Lucena et al. 2011), influenced by the physical characteristics of NEB and planetary-scale atmospheric anomalies (Alizadeh-Choobari 2017). The ENSO (El Niño and La Niña) phenomena and the Atlantic dipole also contribute to modifying the frequency, spatial distribution and intensity of these systems, causing direct changes in rainfall (Acosta-Jamett et al. 2016). Some studies identify semiarid NEB as one of the areas most affected by global climate change (IPCC 2007) and poor water resource management. The expected impacts of climate change on the Brazilian semiarid region include changes in the caatinga vegetation; reduction in water from dams and reservoirs; greater occurrence of dry periods; greater propensity to extreme rains and rains concentrated in a short time period, causing floods; unavailability of subsistence agricultural production; and increased migration.

Figure 7 and Table 3 represent the climatic variability and instability in this region, with successive humid and very dry years. An explanation for these anomalies could be the influence of intense climatic phenomena such as El Niño and La Niña, as presented in the studies by da Silva et al. (2011), Grimm (2011) and Bombardi et al. (2014), who analyzed the influence of ENSO on drought events in NEB. El Niño is an oceanic phenomenon characterized by above-normal warming of surface waters located in the central and eastern Pacific, close to South America, along the coast of Peru, which causes abnormal changes in terrestrial climates that result in severe droughts, floods and cyclones, generating disastrous
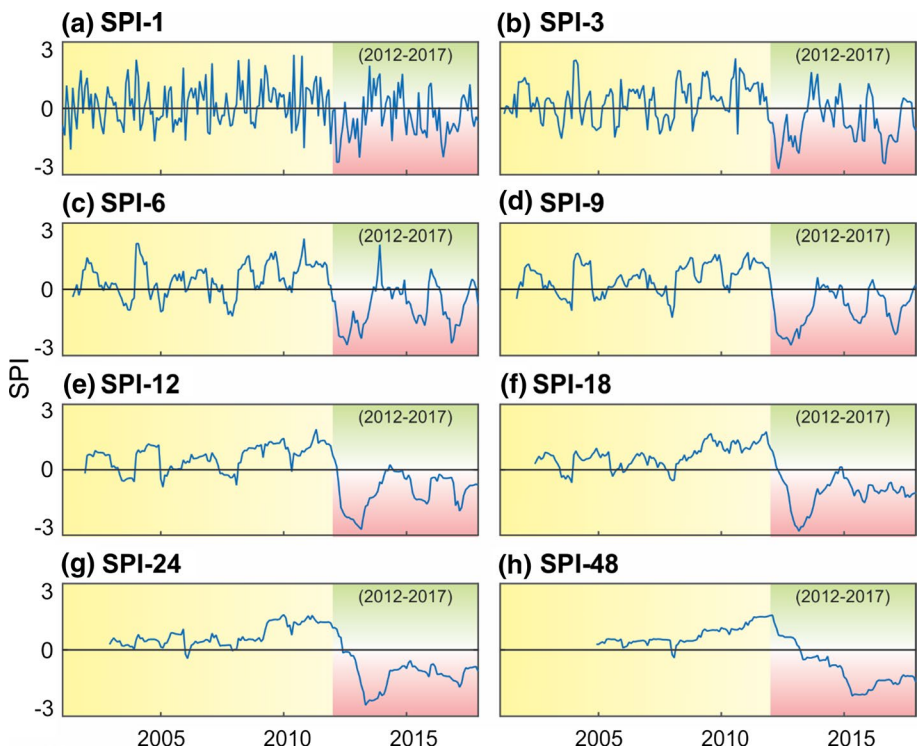

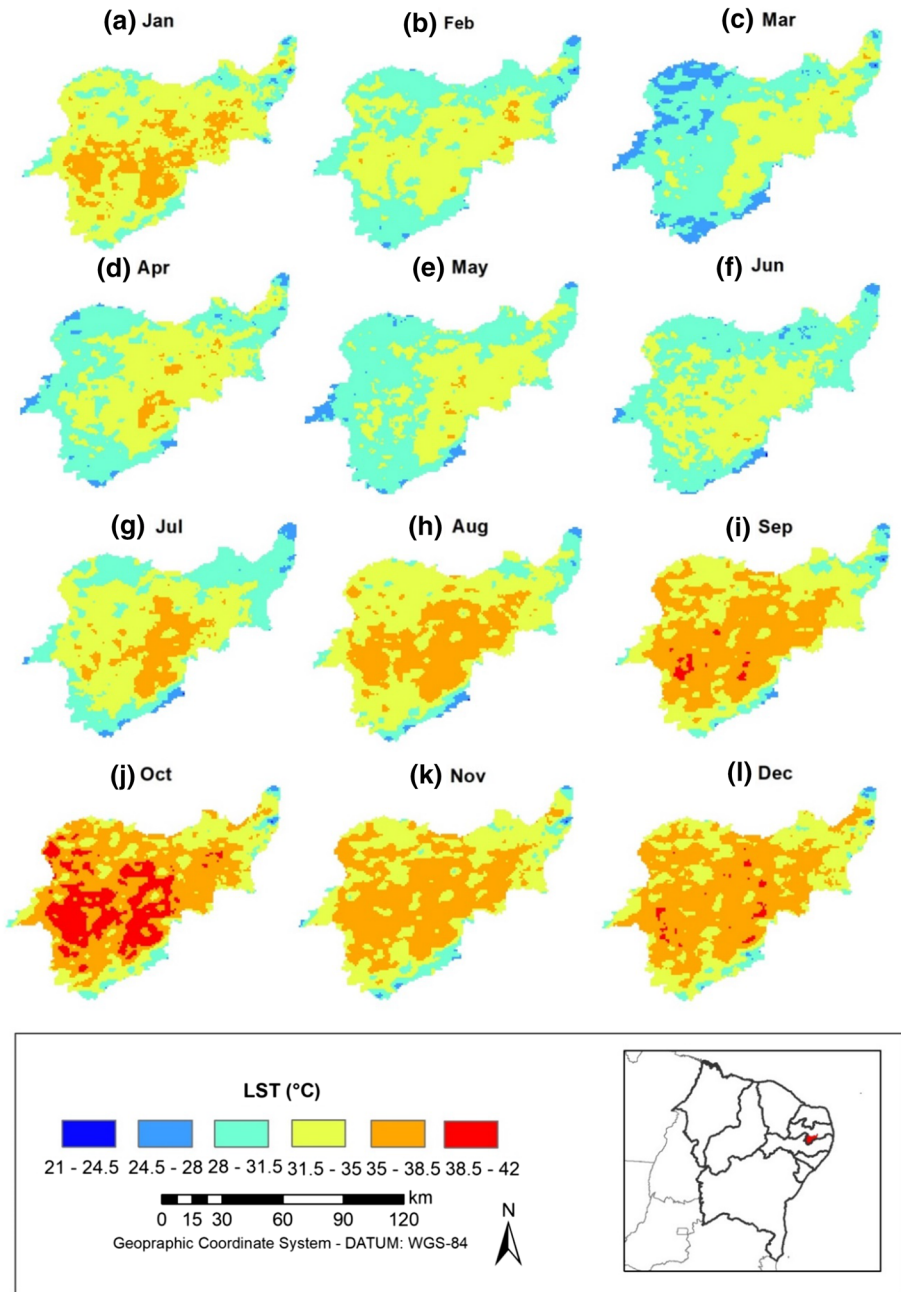Fig. 8 SPI time series for the Upper Paraíba River basin from 2001 to 2017

Fig. 9 Spatial distribution of LST values from 2012 to 2017

societal impacts. According to the Brazilian National Institute of Meteorology, El Niño events occurred in 2014–2015 and 2015–2016 (INMET 2017). However, when analyzing the occurrence of ENSO during the studied period, five of the years classified as being dry were characterized by the occurrence of El Niño, whereas 2012, characterized as being extremely dry, and 2013, characterized as being very dry, presented no correlation with the occurrence of El Niño.

The SPI values for the Upper Paraíba River basin between 2001 and 2017 were computed for all 42 TRMM grid cells. The data were computed using the 1-, 3-, 6-, 9-, 12-, 18-, 24-, 48-month timescales, which are suitable for monitoring short- to long-term water crises. However, Fig. 8 shows the SPI time series based on the mean precipitation over the region, where the period 2012–2017 is highlighted, which is reported as the most severe drought event since 1998 in the Brazilian semiarid region. This figure shows that after 2012, continuous negative SPI values are observed in the long-term analysis (e.g., Fig. 8f–h), which indicates a drought situation. The high variability presented in Fig. 8 is a result of climate change and the water regime in the basin during the analyzed period. Temperature fluctuations above normal climatic conditions and the rainy season with large water deficiencies may have caused this behavior. The results obtained in this study are close to those obtained by Macedo et al. (2010) and Santos et al. (2019a), who analyzed drought events in Paraíba State based on the SPI.

3.2 Analysis of LST behavior

The spatial distribution of LST, shown in Fig. 9, exhibits high values for the study area, ranging from 21 to 42 °C. The month with the lowest average for the period was June with 21 °C, and the highest was December with 42 °C. Regarding the LST behavior from February to June, there is a lower spatial variation in the lower temperatures in the region, which occurs in the higher areas; in areas with water bodies; and in areas with tree vegetation in the basin. In this context, the reduction in vegetation areas on the surface modifies the local microclimatic conditions and directly interferes with the factors that control rainfall and temperature. Figure 9 reveals that a large extension of the study area has high LST values and the lowest values are observed in areas with remnants of large-size vegetation.

Figure 10 illustrates the LST profile for the study area. The results reveal that between 2001 and 2011, there was a variation in LST, but the data did not indicate a trend; however,
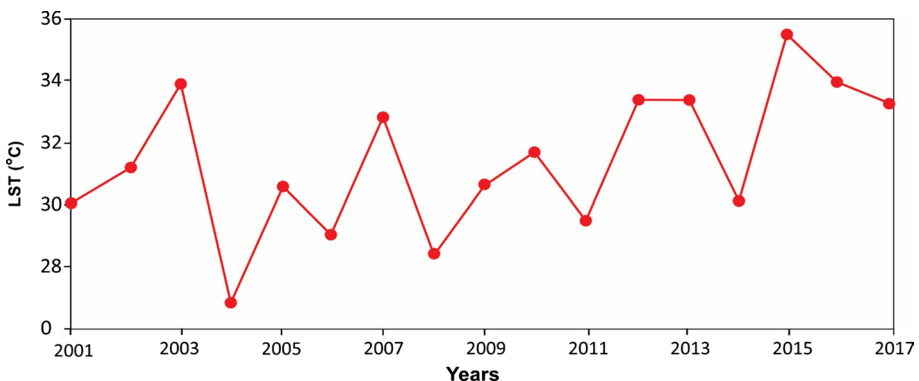

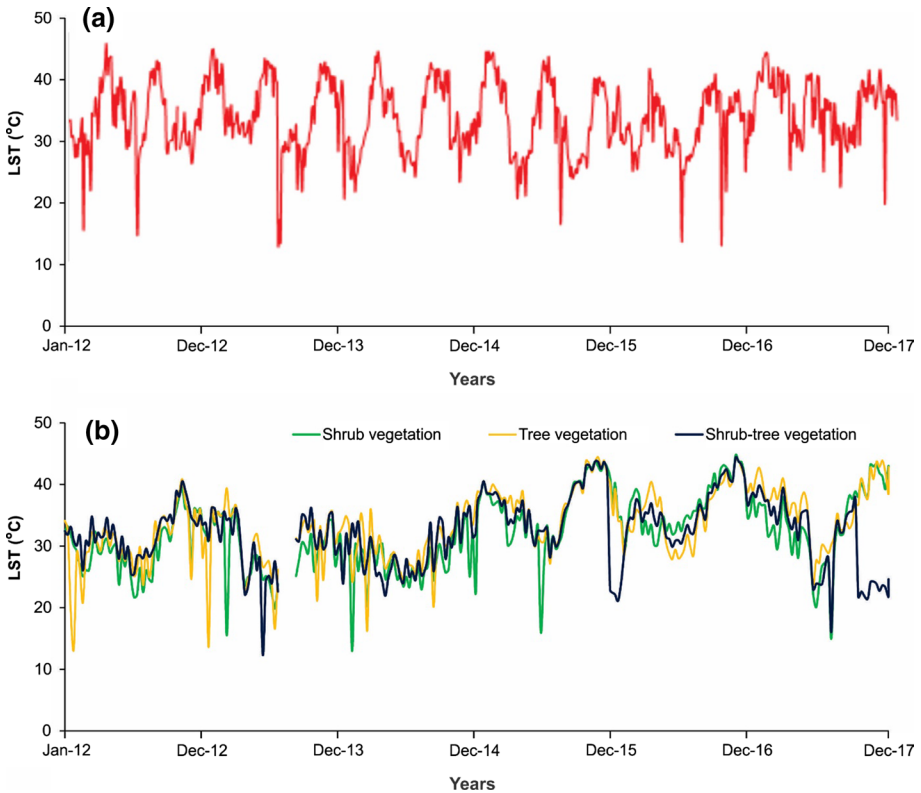**Fig. 10** Estimated annual LST variation between 2001 and 2017

Fig. 11 LST profiles: **a** mean of the study area and **b** for each type of vegetation cover

for the period 2012 to 2017, the results present a positive trend for the LST increase in this part of the Brazilian semiarid region, with a mean annual LST above 32 °C. Figure 11a presents mean LST values for the entire basin. The results highlight that a large part of the basin exhibits LST values above the basin average. This behavior can be explained by the small number of rainfall events in the region, as previously observed in the RAI calculation. Figure 11b presents the LST profiles for each type of vegetation cover analyzed. The results obtained reveal that the mean LST values for the tree, shrub-tree and herbaceous vegetation classes were 30, 31 and 30 °C, respectively. The highest mean deviation values occurred in the herbaceous vegetation class (4.6), followed by tree (4.5) and shrub-tree (4.4) vegetation.

3.3 Spatial–temporal distribution of LAI

LAI is one of the most important biophysical variables that characterize the vegetation and dynamics of a land surface. The spatial–temporal distribution of LAI values in the analyzed period is presented in Fig. 12. Note that the most degraded areas of the basin or those with shrub vegetation are the sites that have the lowest LAI values. The maps show that the monthly LAI behavior between August and January is more homogeneous and presents the lowest values, ranging from 0 to 3. In contrast, between February and July
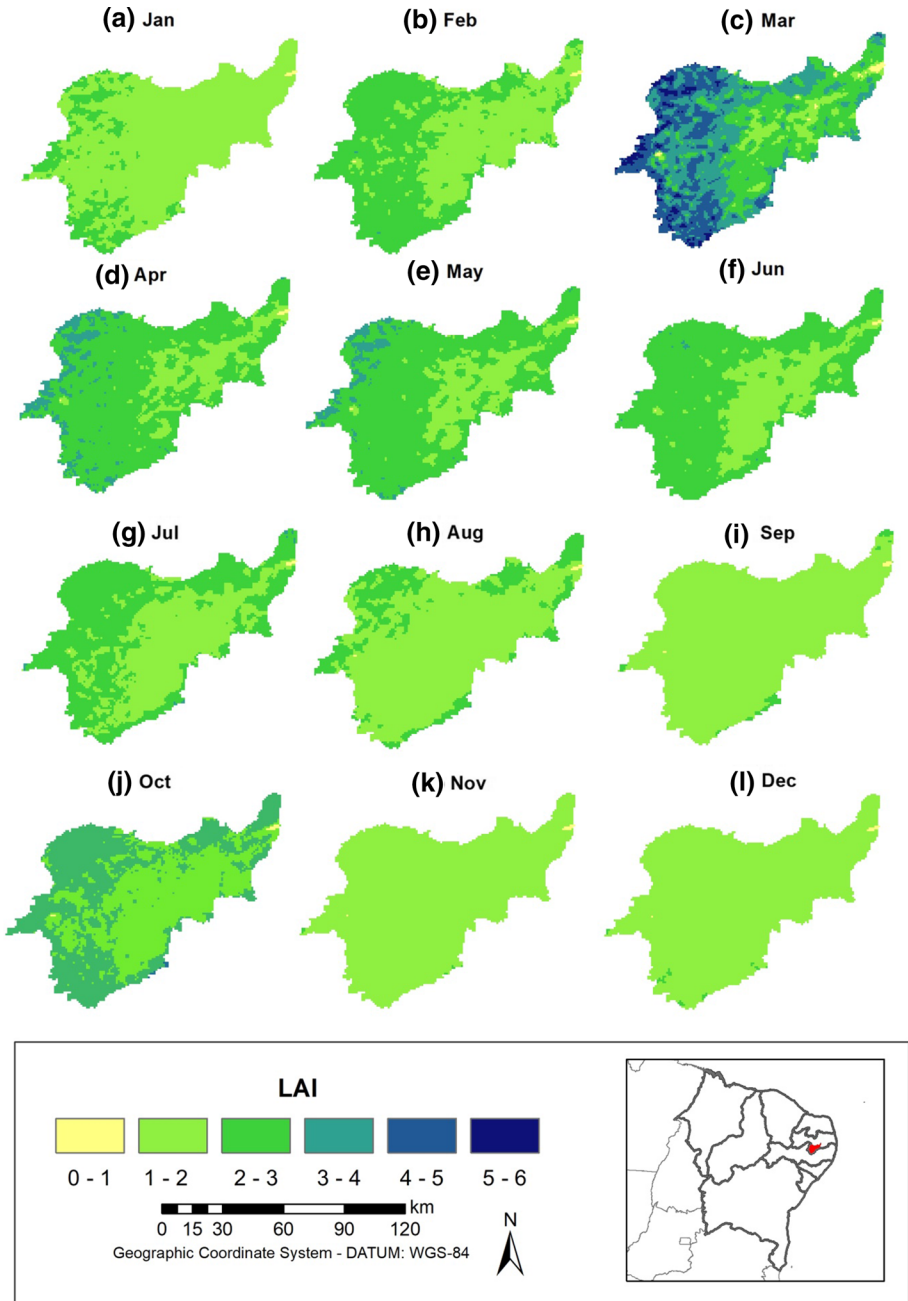
Fig. 12 Spatial distribution of LAI in the study area from 2000 to 2015
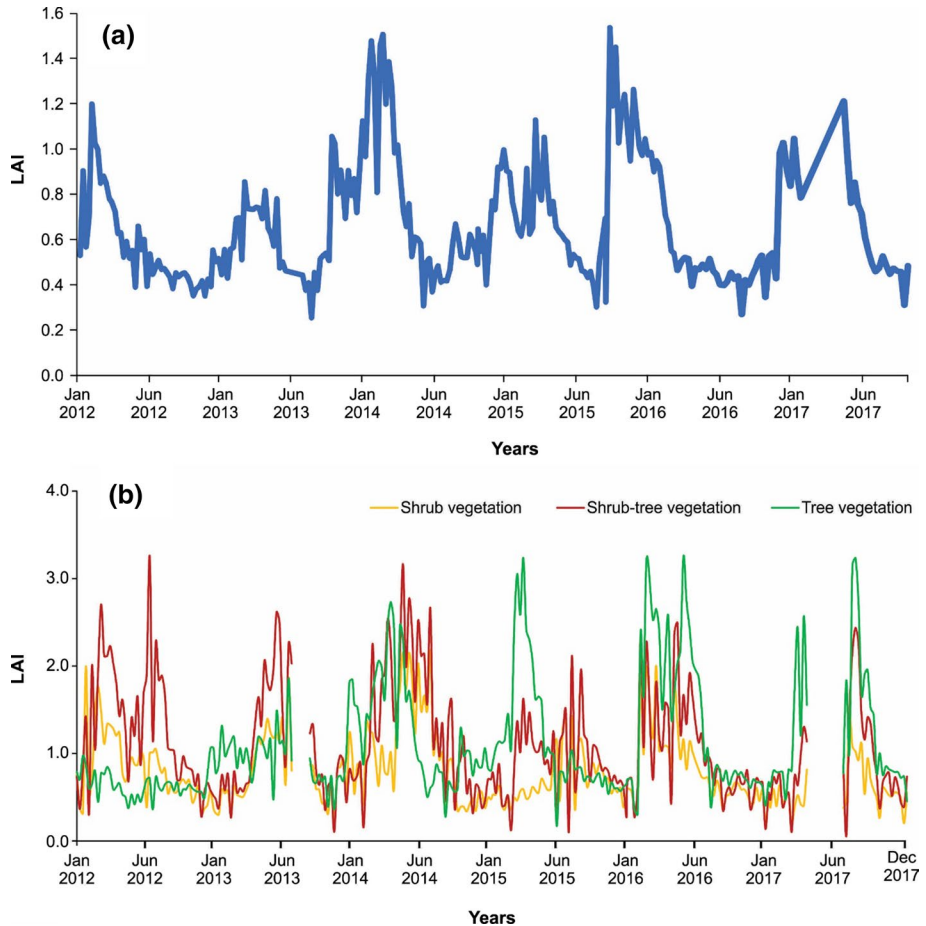
Fig. 13 **a** LAI profile for the study area and **b** LAI profiles for the sample areas (caatinga typologies)

there is a greater variation of LAI values, whereas March exhibits the highest values of this biophysical parameter (4–6) due to the highest historical precipitation values, as shown in Fig. 2b. Moreover, during the driest months, there is a reduction in water in the vegetation, which indicates a hydrological stress due to a drought situation (Panday et al. 2015; Gomes et al. 2017). Precipitation events during drought cycles associated with global solar radiation in semiarid environments influence surface warming, evapotranspiration and the seasonal dynamics of leaf area variations. According to Bezerra et al. (2015), vegetation cover under water stress tends to absorb less solar radiation, which increases its reflection in the visible and absorbs more in the infrared, causing lower vegetation indices, for example, the NDVI and higher surface temperatures.

Observing the spatialization of the LAI in the analyzed period, a decrease in the western portion of the basin is observed during the dry months. The few areas that continue to have high levels of LAI, even during the dry period, have tree vegetation, and some are private areas or environmental protection areas, such as the Jaguar Environmental Protection Area and Cariri Environmental Protection Area. This type of vegetation does
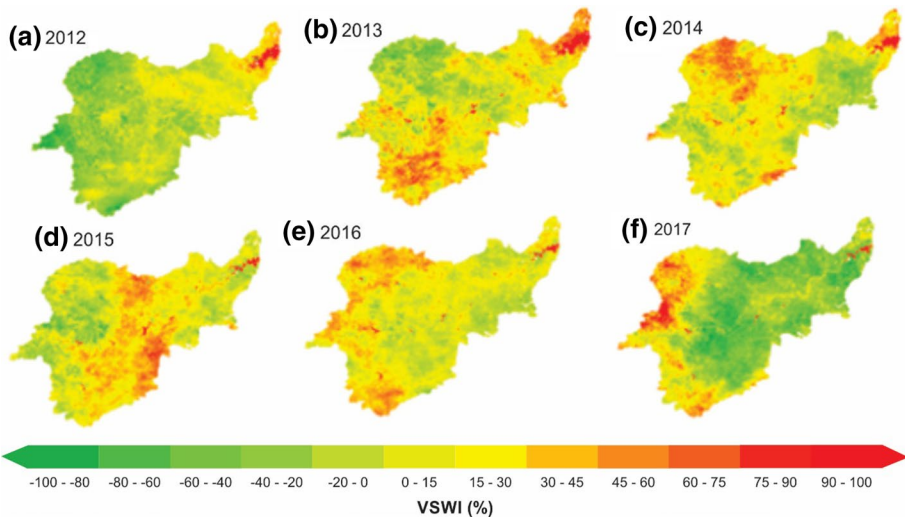
Fig. 14 Annual mean VSWI for Upper Paraíba River basin

not lose leaves, even during periods considered to be dry, but does exhibit a lower biomass density as the rainy period concludes.

As for Fig. 13a, for the mapped regions, the mean LAI values ranged from approximately 0.4 to 2.4. In the Upper Paraíba River basin, historically some areas have exhibited evident signs of desertification, such as the absence of vegetation, exposed soils and areas with a high degree of erosion. Figure 13b presents the LAI profiles for the sampled areas of the caatinga typologies analyzed for the study area. These results exhibit the expected behavior for the period because the shrub and shrub-tree vegetation develop faster and have a higher LAI coinciding with the first rainfall events. As the transition period between the rainy and dry seasons (July and August) begins, there is a decrease in LAI (leaves fall and turn yellow), lowering the biomass level. Tree vegetation clearly presents a decrease in LAI values; however, this type of vegetation is known to maintain vegetative vigor for longer periods. The results also indicate that LAI values are considered high for caatinga vegetation when compared to the results for similar regions obtained by Liu et al. (2010) and Barbosa et al. (2015), who observed a decrease in vegetation vigor in this region.

3.4 Evaluation of VSWI as an indicator of drought

Figure 14 presents the spatial–temporal distribution of the mean annual VSWI for the Upper Paraíba River basin. This figure also indicates that the study area experienced drought conditions during the 2012–2017 study period. As shown in the VSWI anomaly map for the analyzed period, most of the study area in 2013, 2014, 2015 and 2016 exhibited drought conditions. The lowest VSWI values occurred in classes with negative anomaly values, which were primarily in the central and eastern portions of the basin.

The VSWI anomalies in the basin reached approximately − 25%, indicating humid conditions in some parts of the basin. This condition is consistent with the mean annual rainfall in some parts of the basin, primarily during 2012 and 2017, which marks the beginning
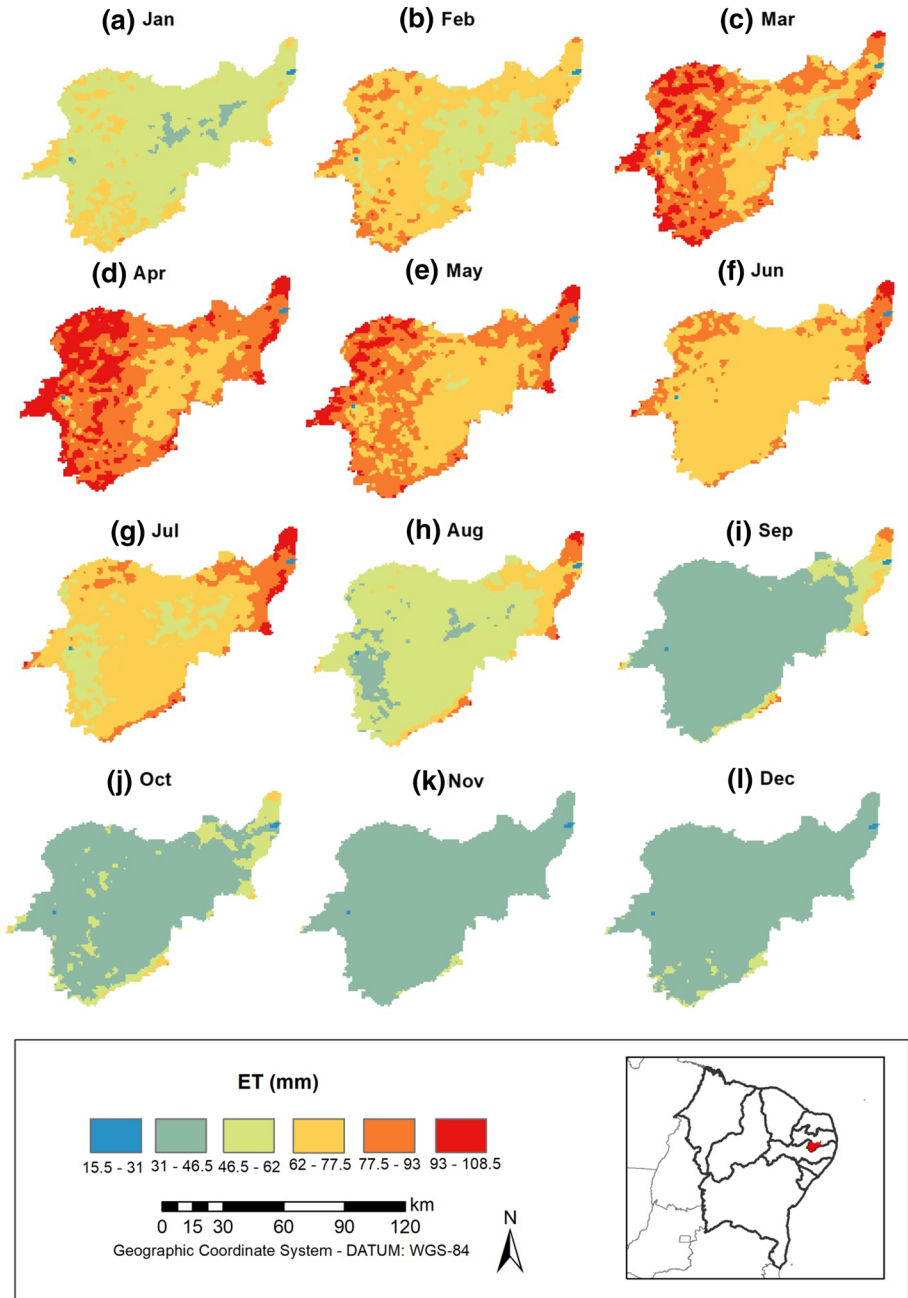
Fig. 15 Spatial distribution of evapotranspiration (ET) in the study area from 2012 to 2017

and end of the analyzed drought period. However, according to the VSWI, approximately 50% of this basin suffered from vegetation drought conditions, especially between 2013 and 2016. Based on the annual mean, this period was characterized by high VSWI values

in most of the study area, which contributed to intense signs of drought in much of the basin, exhibited by vegetation's loss of biomass.

3.5 Monthly variation in ET

Figure 15 depicts the geographic distribution of the monthly mean ET (January–December) in the study area during the drought from 2012 to 2017. In the months considered to be rainy (March to May), the highest ET values are concentrated in the southwestern portion of the basin, which also includes the highest rainfall values according to the spatial distribution of rainfall in the period obtained by Santos et al. (2017) and De Medeiros et al. (2019). Because ET is directly influenced by rainfall, during the dry season of 8 to 10 months, the highest ET values were recorded in the western and eastern portions. The occurrence of these values in the western portion of the basin is due to the presence of the highest areas, for example, Jaguar Environmental Protection Area in São João do Tigre, which has medium to large tree caatinga vegetation and some Atlantic Forest species. The occurrence of higher ET values in the eastern portion, more specifically in the areas near Epitácio Pessoa dam, is due to the agricultural areas that supply many cities in the region.

Estimated ET values reveal that annual values increase in the western and central portions of the basin, reflecting variations in rainfall, available energy and temperature. These ET values at the regional scale are approximately those obtained by Silva et al. (2015) and Santos et al. (2017), who applied the SEBAL algorithm for basins of the semiarid region
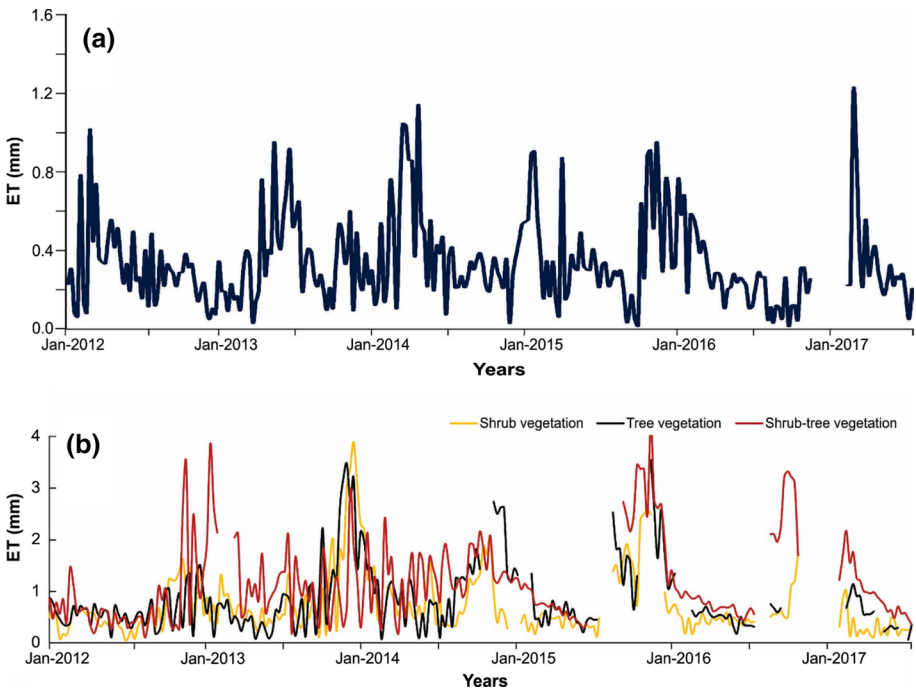

Fig. 16 **a** ET profile for each study area in the analyzed period and **b** ET profiles for three types of vegetation from 2000 to 2017

of Brazil. In other words, the results obtained in this study using the MODIS estimates present ET values in the west that are approximately 1200–1600 mm/year, whereas the minimum rates in the eastern portion are approximately 700 mm/year (Fig. 15).

This close relationship between ET and other climatological parameters can be explained by the fact that the ET process is influenced by the variation in incident solar radiation, a local atmospheric circulation process that regulates the rainfall system, air and soil moisture conditions, and vegetation conditions, which exhibit considerable differences according to the rainy and dry seasons. Overall, actual ET values for the study area ranged from 21 to 138 mm/month. The month with the highest value was April 2013, with 138 mm/day, and the lowest observed value was 23.1 mm/month, in October 2012. Figure 16a presents the ET profile for the entire study area, whereas Fig. 16b shows the ET seasonality for three types of vegetation during the analyzed period, with both panels presenting the ET seasonality during the period.

4 Conclusion

In this study, the objective was to analyze the spatial–temporal variability in vegetation dynamics during the drought period from 2012 to 2017 on a monthly and annual scale within the Upper Paraíba River basin based on MODIS images. It was concluded that although rainfall can be considered the dominant causative factor in the behavior of vegetation growth at the large scale, land use and land cover changes may be the key factors for smaller-scale microclimates.

The behavior of the analyzed variables (LST, LAI and ET) revealed how much vegetation is influenced by rainfall variability in the semiarid region of Brazil. The spatialization of the values exhibited a strong seasonal pattern of the analyzed variables, in which the highest ET values were found in areas known to have remnants of tree-size caatinga vegetation from the period considered rainy. The lowest LAI values were observed in the most degraded areas of the basin, supported by previous studies conducted in the Upper Paraíba River basin with the use of other sensors (De Medeiros et al. 2019; Silva et al. 2018).

An analysis of the temporal profiles of each variable in the caatinga sample areas (shrub vegetation, shrub-tree vegetation and tree vegetation) revealed that the caatinga typology can influence the values of each variable; the shrub and shrub-tree caatinga vegetation are the most influenced in the transition period. The study demonstrated that the Upper Paraíba River basin is severely affected by water stress conditions. However, it was also observed that the drought dynamics indicate erratic behavior, i.e., characterized by several dry and extremely dry years, which has serious implications for water resource management in the region and the development of public policies combating droughts in the region. It can also be concluded that drought reduces vegetation resilience, making plants more vulnerable to the recurrent disturbances mentioned in this study, as depicted in the monthly VSWI maps. Thus, vegetation is severely affected by rainfall variability and, in cases of continuous severely dry years, economic and social problems can affect the local population.

The MODIS LST and ET products presented satisfactory results; however, the LAI products presented overestimated values for the biome analyzed in the dry period. Nevertheless, the results obtained using the MODIS sensor demonstrate that the use of time series to understand biophysical variables is a safe way to monitor and analyze the environmental behavior of a semiarid basin based on a relatively limited amount of data series obtained through weather stations and equipment.

The RAI and SPI were effective in representing the dry and extremely dry years in the analyzed period. Finally, the vegetation dynamics during the dry season were influenced by rainfall, but the VSWI results showed that even in dry years, vegetation in the region was influenced by other factors, such as the hydrodynamic properties of the soil and the phenology of the caatinga biome's vegetation.

Finally, this study is important for the region because the application of these vegetation indices and ET helps identify areas of degradation within the basin and can be used to identify the behavior of vegetative vigor in different typologies of vegetation cover of the Brazilian semiarid region during extreme drought events, as the drought occurred from 2012 to 2017. Thus, this study could be used by decision makers to address natural hazards caused by the intensification of drought periods within this basin and to better manage water resources to develop the Upper Paraíba River basin.

References

Acosta-Jamett G, Gutiérrez JR, Kelt DA, Meserve PL, Previtali MA (2016) El Niño southern oscillation drives conflict between wild carnivores and livestock farmers in a semiarid area in Chile. J Arid Environ 126:76–80. https://doi.org/10.1016/j.jaridenv.2015.08.021

Alizadeh-Choobari O (2017) Contrasting global teleconnection features of the eastern Pacific and central Pacific El Niño events. Dyn Atmos Oceans 80:139–154. https://doi.org/10.1016/j.dynatmoce.2017.10.004

Alvalá RCS, Cunha AP, Brito SB, Seluchi ME, Marengo JA, Moraes OLL, Carvalho MA (2017) Drought monitoring in the Brazilian Semiarid region. Anais da Academia Brasileira de Ciências. https://doi.org/10.1590/0001-3765201720170209

Alvares CA, Stape JL, Sentelhas PC, de Moraes Gonçalves JL, Sparovek G (2013) Köppen's climate classification map for Brazil. Meteorol Z 22(6):711–728. https://doi.org/10.1127/0941-2948/2013/0507

Anderson MC, Zolin CA, Sentelhas PC, Hain CR, Semmens K, Tugrul Yilmaz M, Gao F, Otkin JA, Tetrault R (2016) The Evaporative Stress Index as an indicator of agricultural drought in Brazil: an assessment based on crop yield impacts. Remote Sens Environ 174:82–99. https://doi.org/10.1016/j.rse.2015.11.034

Awange JL, Mpelasoka F, Goncalves RM (2016) When every drop counts: analysis of droughts in Brazil for the 1901–2013 period. Sci Total Environ 566–567:1472–1488. https://doi.org/10.1016/j.scitotenv.2016.06.031

Barbosa HA, Lakshmi Kumar TV, Silva LRM (2015) Recent trends in vegetation dynamics in the South America and their relationship to rainfall. Nat Hazards 77(2):883–899. https://doi.org/10.1007/s11069-015-1635-8

Beuchle R, Grecchi RC, Shimabukuro YE, Seliger R, Eva HD, Sano E, Achard F (2015) Land cover changes in the Brazilian Cerrado and Caatinga biomes from 1990 to 2010 based on a systematic remote sensing sampling approach. Appl Geogr 58:116–127. https://doi.org/10.1016/j.apgeog.2015.01.017

Bezerra BG, Silva BB, Santos CAC, Bezerra JR (2015) Actual evapotranspiration estimation using remote sensing: comparison of SEBAL and SSEB approaches. Adv Remote Sens 4(3):234–247. https://doi.org/10.4236/ars.2015.43019

Bombardi RJ, Carvalho LMV, Jones C, Reboita MS (2014) Precipitation over eastern South America and the South Atlantic Sea surface temperature during neutral ENSO periods. Clim Dyn 42(5–6):1553–1568. https://doi.org/10.1007/s00382-013-1832-7

Brazil Ministry of National Integration (2017) Nova delimitação do semi-árido brasileiro. Resolução Nº 115, de 23 de Novembro de 2017, Brasília

Brito SSB, Cunha APMA, Cunningham CC, Alvalá RC, Marengo JA, Carvalho MA (2018) Frequency, duration and severity of drought in the Semiarid Northeast Brazil region. Int J Climatol 38(2):517–529. https://doi.org/10.1002/joc.5225

Carlson TN, Gillies RR, Perry EM (1994) A method to make use of thermal infrared temperature and NDVI measurements to infer surface soil water content and fractional vegetation cover. Remote Sens Rev 9(1–2):161–173. https://doi.org/10.1080/02757259409532220

Cleugh HA, Leuning R, Mu QZ, Running SW (2007) Regional evaporation estimates from flux tower and MODIS satellite data. Remote Sens Environ 106(3):285–304. https://doi.org/10.1016/j.rse.2006.07.007

Cunha APM, Alvalá RC, Nobre CA, Carvalho MA (2015) Monitoring vegetative drought dynamics in the Brazilian semiarid region. Agric For Meteorol 214–215:494–505. https://doi.org/10.1016/j.agrformet.2015.09.010

Cunha APMA, Barros SS, Rossato L, Alvalá RC, Carvalho MA, Zeri LMM, Cunningham C, Maciel APR, Andrade ES, Vieira RMSP (2017) Avaliação de indicador para o monitoramento dos impactos da seca em áreas de pastagens no semiárido do Brasil. Revista Brasileira de Cartografia 69(1):89–106

da Silva GAM, Drumond A, Ambrizzi T (2011) The impact of El Niño on South American summer climate during different phases of the Pacific Decadal Oscillation. Theor Appl Climatol 106(3–4):307–319. https://doi.org/10.1007/s00704-011-0427-7

Dantas JC, Silva MA, Silva RM, Vianna PCG (2015) Simulação vazão-erosão usando o modelo SWAT para uma grande bacia da região semiárida da Paraíba. Geociências 34(4):816–827

De Azevedo SC, Cardim GP, Puga F, Singh RP, da Silva EA (2018) Analysis of the 2012–2016 drought in the northeast Brazil and its impacts on the Sobradinho water reservoir. Remote Sens Lett 9(5):438–446. https://doi.org/10.1080/2150704X.2018.1437290

De Medeiros IC, da Costa SJFCB, Silva RM, Santos CAG (2019) Run-off-erosion modelling and water balance in the Epitácio Pessoa Dam river basin, Paraíba State in Brazil. Int J Environ Sci Technol 16(7):3035–3048. https://doi.org/10.1007/s13762-018-1940-3

Diniz AS, Paz AR, Allasia DG (2016) Assessment of rainfall estimates of TRMM satellite on Paraíba state. Braz J Water Resour 21(2):288–299. https://doi.org/10.21168/rbrh.v21n2.p288-299

Fang J, Yang W, Luan Y, Du J, Lin A, Zhao L (2019) Evaluation of the TRMM 3B42 and GPM IMERG products for extreme precipitation analysis over China. Atmos Res 223:24–38. https://doi.org/10.1016/j.atmosres.2019.03.001

Gadelha AN, Coelho VHR, Xavier AC, Barbosa LR, Melo DCD, Xuan X, Huffman GJ, Petersen WA, Almeida CN (2019) Grid box-level evaluation of IMERG over Brazil at various space and time scales. Atmos Res 218:231–244. https://doi.org/10.1016/j.atmosres.2018.12.001

García-León D, Contreras S, Hunink J (2019) Comparison of meteorological and satellite-based drought indices as yield predictors of Spanish cereals. Agric Water Manag 213:388–396. https://doi.org/10.1016/j.agwat.2018.10.030

Gomes ACC, Bernardo N, Alcântara E (2017) Accessing the southeastern Brazil 2014 drought severity on the vegetation health by satellite image. Nat Hazards 89(3):1401–1420. https://doi.org/10.1007/s11069-017-3029-6

Grimm AM (2011) Interannual climate variability in South America: impacts on seasonal precipitation, extreme events, and possible effects of climate change. Stoch Environ Res Risk Assess 25(4):537–554. https://doi.org/10.1007/s00477-010-0420-1

Gutiérrez APA, Engle NL, De Nys E, Molejón C, Martins ES (2014) Drought preparedness in Brazil. Weather Clim Extrem 3(1):95–106. https://doi.org/10.1016/j.wace.2013.12.001

Heinemann AB, Ramirez-Villegas J, Stone LF, Didonet AD (2017) Climate change determined drought stress profiles in rainfed common bean production systems in Brazil. Agric For Meteorol 246:64–77. https://doi.org/10.1016/j.agrformet.2017.06.005

Huffman GJ, Bolvin DT (2017) TRMM and other data precipitation data set documentation. Global Change Master Directory, NASA, p 45

Hunt JD, Stilpen D, de Freitas MAV (2018) A review of the causes, impacts and solutions for electricity supply crises in Brazil. Renew Sustain Energy Rev 88:208–222. https://doi.org/10.1016/j.rser.2018.02.030

INMET (2017). Instituto Nacional de Meteorologia. Accessed 06 Oct 2018 https://www.inmet.gov.br/portal/index.php?r=clima/desvioChuvaTrimestral

International Panel on Climate Change (IPCC) (2007) Climate Change 2007: synthesis report: summary for policymakers, contribution of working groups I-III to the Fourth Assessment Report of the Intergovernmental Panel on Climate Change. Cambridge University Press, Cambridge, p 2007

Jiang B, Liang S, Wang J, Xiao Z (2010) Modeling MODIS LAI time series using three statistical methods. Remote Sens Environ 114(7):1432–1444. https://doi.org/10.1016/j.rse.2010.01.026

Kalimeris A, Kolios S (2019) TRMM-based rainfall variability over the Central Mediterranean and its relationships with atmospheric and oceanic climatic modes. Atmos Res 230:104649. https://doi.org/10.1016/j.atmosres.2019.104649

Kraus EB (1977) Subtropical droughts and cross-equatorial energy transports. Mon Weather Rev 105(8):1009–1018. https://doi.org/10.1175/1520-0493(1977)105%3c1009:SDACEE%3e2.0.CO;2

Kummerow C, Barnes W, Kozu T, Shiue J, Simpson J (1998) The tropical rainfall measuring mission (TRMM) sensor package. J Atmos Oceanic Technol 15(3):809–817

Kummerow C, Simpson J, Thiele O, Barnes W, Chang AT, Stocker E, Adler RF, Hou A, Kakar R, Wentz F, Ashcroft P, Kozu T, Hong Y, Okamoto K, Iguchi T, Kuroiwa H, Im E, Haddad Z, Huffman G, Ferrier B, Olson WS, Zipser E, Smith EA, Wilheit TT, North G, Krishnamurti T, Nakamura K (2000) The status of the tropical rainfall measuring mission (TRMM) after two years in orbit. J Appl Meteorol 39:1965–1982. https://doi.org/10.1175/1520-0450(2001)040%3c1965:TSOTTR%3e2.0.CO;2

Li X, Du H, Mao F, Zhou G, Han N, Xu X, Liu Y, Zhu D, Zheng J, Dong L, Zhang M (2019) Assimilating spatiotemporal MODIS LAI data with a particle filter algorithm for improving carbon cycle simulations for bamboo forest ecosystems. Sci Total Environ 694:133803. https://doi.org/10.1016/j.scitotenv.2019.133803

Liu S, Liu R, Liu Y (2010) Spatial and temporal variation of global LAI during 1981–2006. J Geogr Sci 20(3):323–332. https://doi.org/10.1007/s11442-010-0323-6

Lucena DB, Servain J, Gomes Filho MF (2011) Rainfall response in northeast Brazil from ocean climate variability during the second half of the twentieth century. J Clim 24(23):6174–6184. https://doi.org/10.1175/2011JCLI4194.1

Ma T, Duan Z, Li R, Song X (2019) Enhancing SWAT with remotely sensed LAI for improved modelling of ecohydrological process in subtropics. J Hydrol 570:802–815. https://doi.org/10.1016/j.jhydrol.2019.01.024

Macedo MJH, Guedes RVS, Sousa FAS, Dantas FR (2010) Analysis of the standardized precipitation index for the Paraíba state, Brazil. Revista Ambientee Água 5(1):204–214. https://doi.org/10.4136/ambi-agua.130

Marengo JA, Alves LM, Alvalá RCS, Cunha APMA, Brito SSB, Moraes OLL (2017) Climatic characteristics of the 2010–2016 drought in the semiarid Northeast Brazil region. Anna Braz Acad Sci 90(2):1–21. https://doi.org/10.1590/0001-3765201720170206

Mariano DA, dos Santos CAC, Wardlow BD, Anderson MC, Schiltmeyer AV, Tadesse T, Svoboda MD (2018) Use of remote sensing indicators to assess effects of drought and human-induced land degradation on ecosystem health in Northeastern Brazil. Remote Sens Environ 213:129–143. https://doi.org/10.1016/j.rse.2018.04.048

Mckee T, Doesken N, Kleist J (1993) The relationship of drought frequency and duration to time scales. in: Proceedings of the 8th Conference on Applied Climatology, American Meteorological Society, Boston, MA

Myneni RB, Hoffman S, Knyazikhin Y, Privette JL, Glassy J, Tian Y, Wang Y, Song X, Zhang Y, Smith GR, Lotsch A, Friedl M, Morisette JT, Votava P, Nemani RR, Running SW (2002) Global products of vegetation leaf area and fraction absorbed PAR from year one of MODIS data. Remote Sens Environ 83:214–231. https://doi.org/10.1016/S0034-4257(02)00074-3

Panday PK, Coe MT, Macedo MN, Lefebvre P, Castanho ADA (2015) Deforestation offsets water balance changes due to climate variability in the Xingu River in eastern Amazonia. J Hydrol 523:822–829. https://doi.org/10.1016/j.jhydrol.2015.02.018

Santos CAG, Brasil Neto RM, da Silva RM, Dos Santos DC (2019a) Innovative approach for geospatial drought severity classification: a case study of Paraíba state, Brazil. Stoch Env Res Risk Assess 33(2):545–562. https://doi.org/10.1007/s00477-018-1619-9

Santos CAG, Brasil Neto RM, da Silva RM, Costa SGF (2019b) Cluster analysis applied to spatiotemporal variability of monthly precipitation over Paraíba state using tropical rainfall measuring mission (TRMM) data. Remote Sens 11(6):637. https://doi.org/10.3390/rs11060637

Santos CAG, Silva RM, Silva AM, Brasil Neto RM (2017) Estimation of evapotranspiration for different land covers in a Brazilian semi-arid region: a case study of the Brígida River basin, Brazil. J S Am Earth Sci 74(1):54–66. https://doi.org/10.1016/j.jsames.2017.01.002

Santos CAG, Brasil Neto RM, Silva RM, Passos JSA (2018) Integrated spatiotemporal trends using TRMM 3B42 data for the Upper São Francisco River basin. Brazil Environ Monit Assess 190:175. https://doi.org/10.1007/s10661-018-6536-3

Silva AM, Silva RM, Silva BB (2015) Determinação de temperatura da superfície, saldo de radiação e evapotranspiração usando imagens Landsat e dados observados. Braz J Cartogr 67(4):1203–1216

Silva RM, Santos CAG, Maranhão KUA, Silva AM, Lima VRP (2018) Geospatial assessment of eco-environmental changes in desertification area of the Brazilian semi-arid region. Earth Sci Res J 22(3):175–186. https://doi.org/10.15446/esrj.v22n3.69904

Silva JFCBC (2019). Crise hídrica no abastecimento de água em Campina Grande: análise de cenários futuros no volume de água no reservatório Epitácio Pessoa entre 2020–2030. Ph.D. Thesis in Geography, Universidade Federal da Paraíba, p 120.

Van Rooy MP (1965) A rainfall anomaly index independent of time and space. Notos 1965(14):43p

Xiao ZQ, Liang SL, Wang JD, Song JL, Wu XY (2009) A temporally integrated inversion method for estimating Leaf Area Index from MODIS data. IEEE Trans Geosci Remote Sens 47(8):2536–2545. https://doi.org/10.1109/TGRS.2009.2015656

Xie X, Li A, Jin H, Tan J, Wang C, Lei G, Zhang Z, Bian J, Nan X (2019) Assessment of five satellite-derived LAI datasets for GPP estimations through ecosystem models. Sci Total Environ 690:1120–1130. https://doi.org/10.1016/j.scitotenv.2019.06.516

Zhou L, Wu J, Zhang J, Leng S, Liu M, Zhao L, Zhang F, Shi Y (2013) The integrated surface drought index (ISDI) as an indicator for agricultural drought monitoring: theory, validation, and application in Mid-Eastern China. IEEE J Sel Top Appl Earth Observ Remote Sens 6:1254–1262. https://doi.org/10.1109/JSTARS.2013.2248077

Publisher's Note Springer Nature remains neutral with regard to jurisdictional claims in published maps and institutional affiliations.